TN 66-44
H. Brechna
October 1966

EDDY CURRENT LOSSES IN THE SLAC ONE-METER LIQUID HYDROGEN BUBBLE CHAMBER PISTON

ABSTRACT

Eddy current losses due to piston movements in an inhomogeneous magnetic field are calculated. The axial and radial magnetic field components are determined using SLAC NUTCRACKER program. With the actual piston displacement of 0-0.52-0 cm in 22×10^{-3} sec, peak losses of 950 watts are generated in the Kromarc piston. Without the 9% Ni-Fe plate, peak losses in the piston are 400 watts. The losses are mainly concentrated in the areas of the piston facing the magnet pole, close to the piston shaft.

I. INTRODUCTION

The SLAC one-meter liquid hydrogen bubble chamber is equipped with a moveable backwall coupled to the main chamber body over stainless steel bellows and is activated through hydraulic systems to operate the chamber. The backwall, in this paper called "Piston" for simplicity, moves 0.52 cm from its "dead" position in a time of about 11×10^{-3} seconds and returns to its original position, with the total cycle length for chamber activation of 22×10^{-3} seconds.

The piston is made of Kromarc 55,(W) an alloy with the chemical composition of[1]

C = 0.05%	Mo = 2.15%
Mn = 8.2%	S = 0.012%
Si = 0.22%	P = 0.013%
Cr = 15.43%	Fe = 52.6%
Ni = 21.24%	

The piston surface facing the liquid hydrogen bath is concave and covered with a layer of a reflective film commercially called "Scotchlite" and described by Sukiennicki.[2] The piston moves in a highly inhomogeneous field and the nonuniform heating generated by eddy currents flowing through the piston body due to flux extraction could cause temperature gradients in the liquid hydrogen bath and undesirable boiling.

The field calculation in the chamber was performed using the SLAC NUT-CRACKER program, which is written in Algol. The bubble chamber magnet was assumed to be axially symmetric, in order to make use of the present program which handles only two dimensional Cartesian coordinates and axial symmetric cases. Due to limitations in the computer storage capacity of 16,000 words in the core memory and 32,000 words in the drum, to obtain information for each block a time of 20×10^{-3} sec is needed which, compared to

---

(W) Westinghouse trademark.

[1] Chemical analysis obtained from J. Mark, SLAC.

[2] B. Sukiennicki and H. Barney, "Tests on Scotchlite Placed in a Simulated Hydrogen Chamber," SLAC-PUB-230, International Conference on Instrumentation for High Energy Physics, Stanford Linear Accelerator Center, September 1966.

6×10^{-6} sec from the core reference, is exceedingly long. (We are using B5500 which is more readily available for computation and is slightly cheaper than 7090 and therefore convenient to SLAC .) For a problem of the present size it is preferable not to use the drum and choose the mesh size, which enables the use of the core capacity only. A mesh size of 4×4 cm^2 was adapted in earlier calculations[3] to obtain a first approximation of the field distribution over the whole chamber area. It is obvious that this coarse mesh does not give accurate loss values in the piston and calculation errors in excess of 20% may be expected.

Using the 4×4 cm^2 mesh, the general field shape in the chamber was obtained which allows a definition of the Neumann boundary and cuts the size of the region to be computed in half. With a slight error (the field radial component in the magnet beam entrance plane is maximum 300 gauss), the position of the vertical Neumann boundary was chosen. The region to be calculated needs 75 units in the vertical and 50 units in the horizontal plane with a mesh size of 2.5×2.5 cm^2. The matrix for 3.75×10^3 linear equations and 3.75×10^3 unknowns are solved by an iterative method[4] which uses nearly the total core capacity of the B5500.

The field computation per point needs 225 iterations at each point and is calculated in 16×10^{-3} seconds. The total computation time for each special case (the several cases are described in the following sections) was three hours. After the initial case was calculated, it was used for the other cases as well, without starting over again. (B5500 is a comparatively slow machine. Using 7090, the computation time for each case would be 1.5 to 2 hours).

The calculation method is still regarded as relatively slow, but unfortunately at present, several improvements to speed up the program were not satisfactory and could not be used in the present case.

The field distribution in z and r directions over small piston regions are found to be linear in space, which results in simple calculation results. The

---

[3] H. Brechna, "Magnetic Properties of 9% Nickel Steel at Room and Cryogenic Temperatures," SLAC TN-65-87.

[4] E. Burfine, L. Anderson, H. Brechna, "A Computer Code for Variable Permeability Magnetostatic Field Problems," SLAC Report No. 56 (1966).

piston shape is also approximated for calculation purposes. It is assumed that the errors due to computation and the above-mentioned approximations do not exceed 10%.

From an original shape, the piston has undergone several changes to the present form. The eddy current calculations for these modifications do not appear in this paper.

As seen from Figure 1, the magnet is provided with one pole backing the piston. The axial field distribution is corrected by means of the axial ampere-turn distribution. The calculated axial and radial field distribution (using the 2.5×2.5 cm^2 mesh size) is given in Figures 2a - 2d. The peak axial field on the symmetry axis is about 21 kG. The axial magnetic field homogeneity in the useful chamber region is better than ± 5%.

The use of an additional 9% Ni-Fe plate[3] increases the field level in the chamber from 21.0 kG to 23 kG on the symmetry axis; however, it leads to an axial field distribution which is not compensated by the originally calculated coil MMF distribution. $\left(\frac{\Delta B}{B} = \pm 6\%\right)$. The radial and axial field distribution is less homogeneous over the piston area using the 9% Ni-Steel than the case without the 9% Ni back plate. However, as the computation in Section II shows, the average joule heating values are not excessive and also most of the heat is generated on the back part of the piston not facing the liquid hydrogen. A reduction of the magnet MMF of about 7% (equivalent to 21.5 kG in the chamber) will reduce the losses by another 12% if this is required. Figures 3a and 3b illustrate the axial and radial field distribution over the piston region.

II. AXIAL AND RADIAL FIELD DISTRIBUTION

Assuming axial symmetry and Neumann conditions at 22 cm to the right of the shorter coil section (see Figure 1), the field is calculated in a rectangular mesh set of 2.5×2.5 cm^2.

The field distribution over the piston has been obtained by curve fitting and may be linearized over the region of the piston movements, $0 \leqq z \leqq 0.52$ cm. The piston is divided for calculation purposes in square blocks of 2.5×2.5 cm^2 and the field components calculated in each corner point.

---

[3] op. cit.

The piston movements measured by J. Mark are illustrated in Figure 4 and are approximated by the equation:

$$z = 5.2 \cdot \sin^2\left(\frac{\pi t}{T}\right) \qquad \text{(mm)}$$

The piston retains its original position after $T = 22 \times 10^{-3}$ seconds.

The field gradient in the axial and radial direction is assumed to be constant over each square block. By moving the piston 5.2 mm in the positive z direction, the piston sweeps through a nonuniform field in z and r direction and to calculate the eddy current losses, the total field changes of:

$$\Delta B_z = \left[\Delta B^2_{z,z} + \Delta B^2_{z,r}\right]^{\frac{1}{2}}$$

and

$$\Delta B_r = \left[\Delta B^2_{r,r} + \Delta B^2_{r,z}\right]^{\frac{1}{2}}$$

have been calculated.

To account for the piston shape, the field values in corresponding square blocks have been taken into consideration. The field distribution calculated for the two cases with 9% Ni-Steel ring and without the ring are shown in Figures 3a and 3b. The eddy current loss calculation is rather crude and has an accuracy of about 10%.

A. Losses due to change of the axial field component

Over a mesh of 2.5 cm, the field component B_z changes linearly according to the equation:

$$B_z = B_{z_o} + \frac{\Delta B}{z_o} \cdot z \quad \ldots\ldots \qquad (1)$$

with B_{z_o} the corresponding axial field component at piston position $z = z_o$ prior to movement. z is the actual piston displacement. The piston displacement is given by:

$$z = z_o \cdot \sin^2\left(\frac{\pi t}{T}\right) \quad \ldots\ldots \qquad (2)$$

The field gradient over a block is expressed by:

$$\Delta B_z = \Delta B_o \cdot \sin^2\left(\frac{\pi t}{T}\right) \quad \ldots\ldots \qquad (3)$$

The piston movements generate eddy currents to compensate for the field change. The voltage induced in the piston body is (Fig. 5):

$$\Delta V = \pi r^2 \frac{d(\Delta B)}{dt}$$

$$= \frac{\pi^2 r^2}{T} \Delta B_o \cdot \sin\left(\frac{2\pi t}{T}\right) \quad \ldots\ldots \quad (4)$$

The resistance of an element in the piston of radial width of dr axial thickness of z may be expressed as:

$$dR = \rho \cdot \frac{2\pi r}{z dr} = \rho \cdot \frac{2\pi r}{z_o \sin^2\left(\frac{\pi t}{T}\right) dr} \quad \ldots\ldots \quad (5)$$

and the eddy current losses due to piston movement

$$dP = \frac{(\Delta V)^2}{dR} = \frac{\pi^3 \Delta B_z^2}{2\rho T^2} \cdot \sin^2\left(\frac{2\pi t}{T}\right) \cdot z_o \cdot r^3 dr$$

integrated:

$$P = \frac{\pi^3 (\Delta B_z)^2}{8\rho T^2} \cdot z_o \cdot \sin^2\left(\frac{2\pi t}{T}\right) \cdot \left(R_o^4 - R_i^4\right) \quad \ldots\ldots \quad (6)$$

The peak loss value is arrived at $t = \frac{T}{4}$.

If the piston cross-sectional area is divided into square blocks of pre-chosen dimensions, such as in this case $\Delta R_o = 2.5$ cm $\Delta z_o = 2.5$ cm, the corresponding field gradient ΔB_z is obtained from Fig. 3a and Fig. 3b, we may calculate the peak field for:

$$z_o = 5.2 \times 10^{-3} \text{ m}; \quad T = 22 \times 10^{-3} \text{ sec}; \quad \rho = 75 \times 10^{-8} \text{ ohm} \cdot \text{m}$$

and get the peak loss value to be:

$$\hat{P} = 5.5 \times 10^7 \left(\Delta B_{z_{red}}\right)^2 \times \left(R_o^4 - R_i^4\right) \quad \text{(watts)}$$

with ΔB_z in Vs/m^2 and R_o, R_i in m.

The resistivity of Kromarc 55® has been measured at different temperatures and is given in Fig. 6.

The $\Delta B_{z_{red}}$ values from Figs. 3a and 3b should be reduced linearly to $\frac{5.2}{25} \times \Delta B_z$ in order to obtain the actual field change over the region of the piston movements.

With the B_z numbers from Fig. 3a, the peak losses due to the change in axial field are calculated to be approximately 700 watts. The average loss value for a train of $\cos^2 t$ pulses with a period t_o is given by:[5]

$$P_{av} = \frac{1}{4} \hat{P} \cdot \frac{T}{t_o} \quad \ldots\ldots \tag{7}$$

With one chamber operation per second: ($t_o = 1$ sec)

$$P_{av} \cong 4 \text{ watts}$$

With two chamber operations per second: ($t_o = 0.5$ sec)

$$P_{av} = 8 \text{ watts}$$

B. Losses due to change of the radial field component

As in Section II. A, the field change over a mesh of 2.5×2.5 cm^2 is assumed to be linear and expressed in the form:

$$\Delta B_r = \frac{\Delta B_o}{r_o} \cdot r \cdot \sin^2\left(\frac{\pi t}{T}\right) \ldots\ldots \tag{8}$$

The induced voltage in the piston due to the B_r change is given by:

$$U = 2\pi \int \frac{dB}{dt} \cdot r_o \, dz$$

$$= \frac{2\pi^2}{T} \Delta B_r \cdot \sin\left(\frac{2\pi t}{T}\right) \cdot r \cdot z \quad \ldots\ldots \tag{9}$$

The resistance of an element with the radial width dr and axial thickness z is (Fig. 7):

$$dR = \rho \frac{4\pi r}{z\,dr}$$

---

[5] Reference Data for Radio Engineers, Fourth Edition, ITT Corporation, New York, 1962, p. 1023.

and the losses:

$$P = \frac{\pi^3}{2\rho T^2} \cdot \left(\Delta B_r\right)^2 \cdot \sin^2\left(\frac{2\pi t}{T}\right) \cdot z_o^3 \cdot \left(R_o^2 - R_i^2\right) \ldots\ldots \quad (10)$$

With the data given in II.A, the peak field is calculated from:

$$\hat{P} = 6 \times 10^3 \left(\Delta B_r\right)^2 \cdot \left(R_o^2 - R_i^2\right) \quad \text{(watts)}$$

The losses due to the variation of the radial field component give the value of $\hat{P} = 250$ watts.

The average loss values for the total losses (axial and radial) using (7) are calculated to be:

1 pulse per second operation: $P_{av} = 5.3$ watts

2 pulses per second operation: $P_{av} = 10.6$ watts

Most losses occur in the piston surface area facing the 9% Ni-Fe plate in section 2 of the piston. The losses in the piston facing the liquid hydrogen, adjacent to the Scotchlite surface, are small and may be disregarded.

C. Loss calculation in the piston without the 9% Ni-Fe plate

Removing the 9% Ni-Fe plate and replacing it with a non-ferromagnetic material (Fig. 3a), but not changing the original piston position with regard to the chamber, yields to a peak loss value (axial and radial) of approximately 400 watts. The average and rms loss values are respectively:

1 pulse per second operation: $P_{av} = 2.2$ watts

2 pulses per second operation: $P_{av} = 4.4$ watts

As in case II,B, the loss concentration is again in section 2, facing the 9% Ni-Fe plate.

ACKNOWLEDGEMENT

The author would like to thank J. Mark, E. Burfine, and M. Stangenes, SLAC, for their kind cooperation and stimulating discussions.

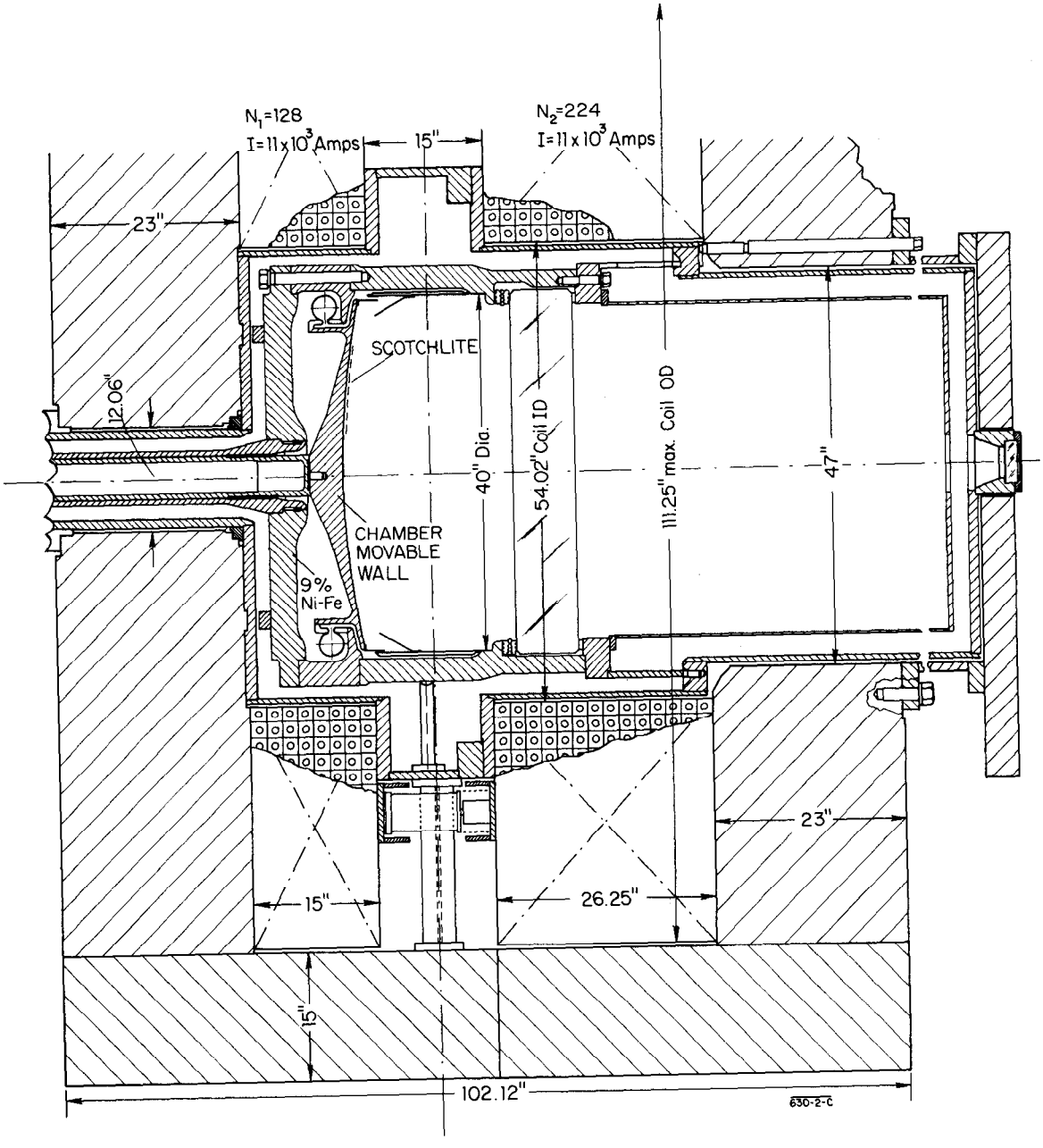

FIG. 1--SLAC 1-meter bubble chamber and magnet assembly.

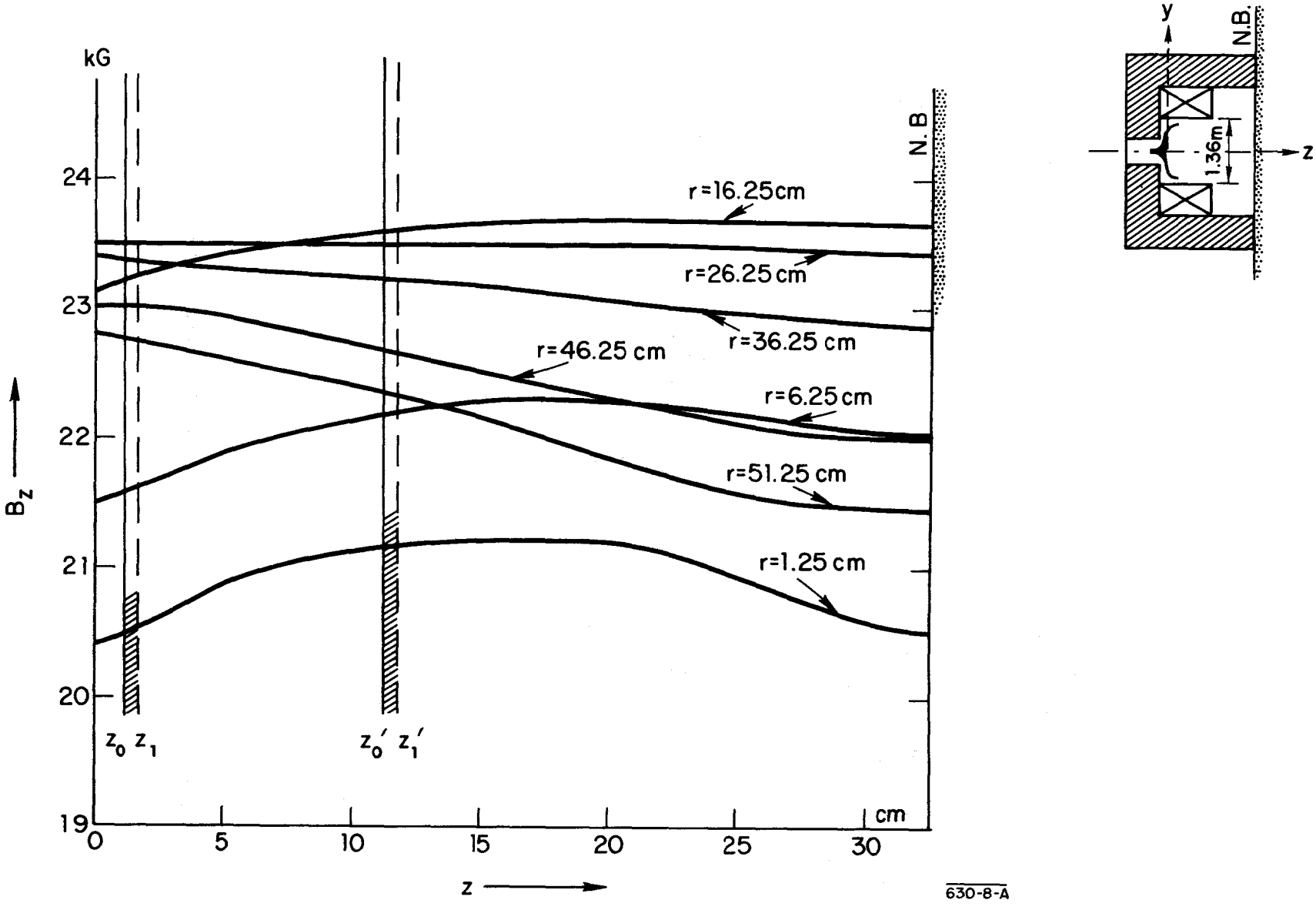

FIG. 2a--Axial field distribution (parameter radial positions). The magnet is without 9% Ni-Fe plate. z_0' and z_1' are the positions of the movable wall during chamber operation.

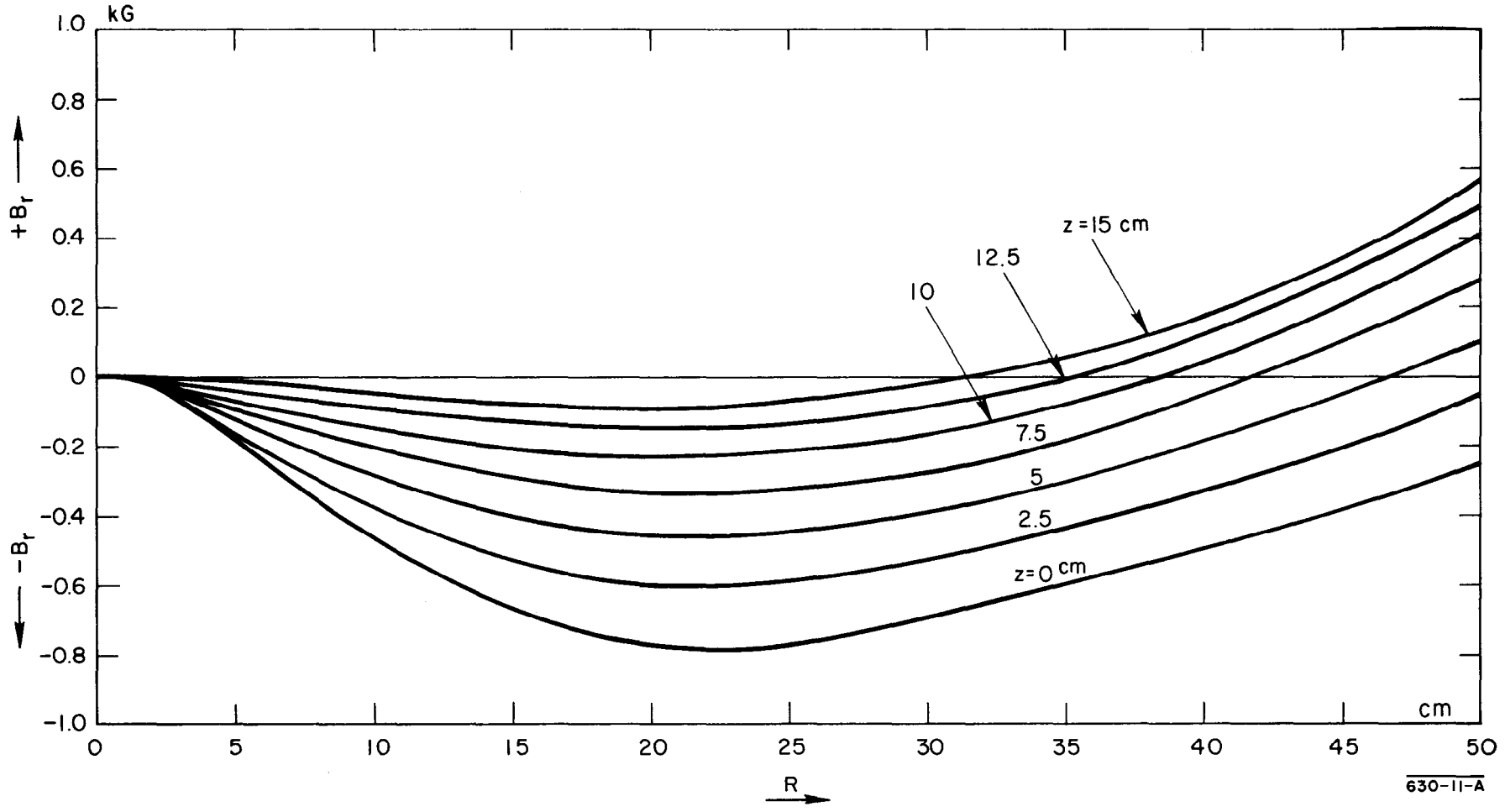

FIG. 2b--Radial field distribution (parameter axial positions).

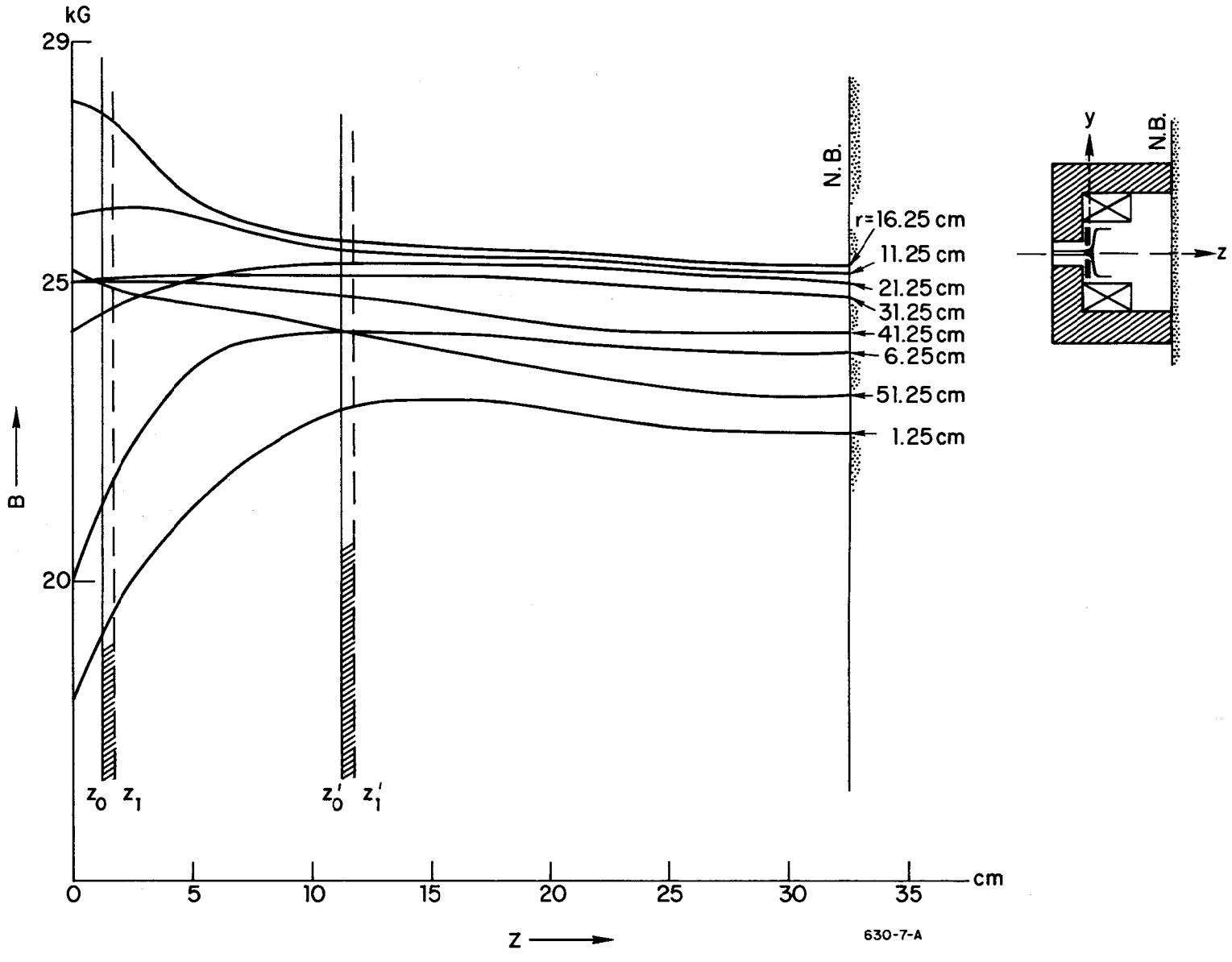

FIG. 2c--Axial field distribution. Magnet provided with 9% Ni-Fe plate.

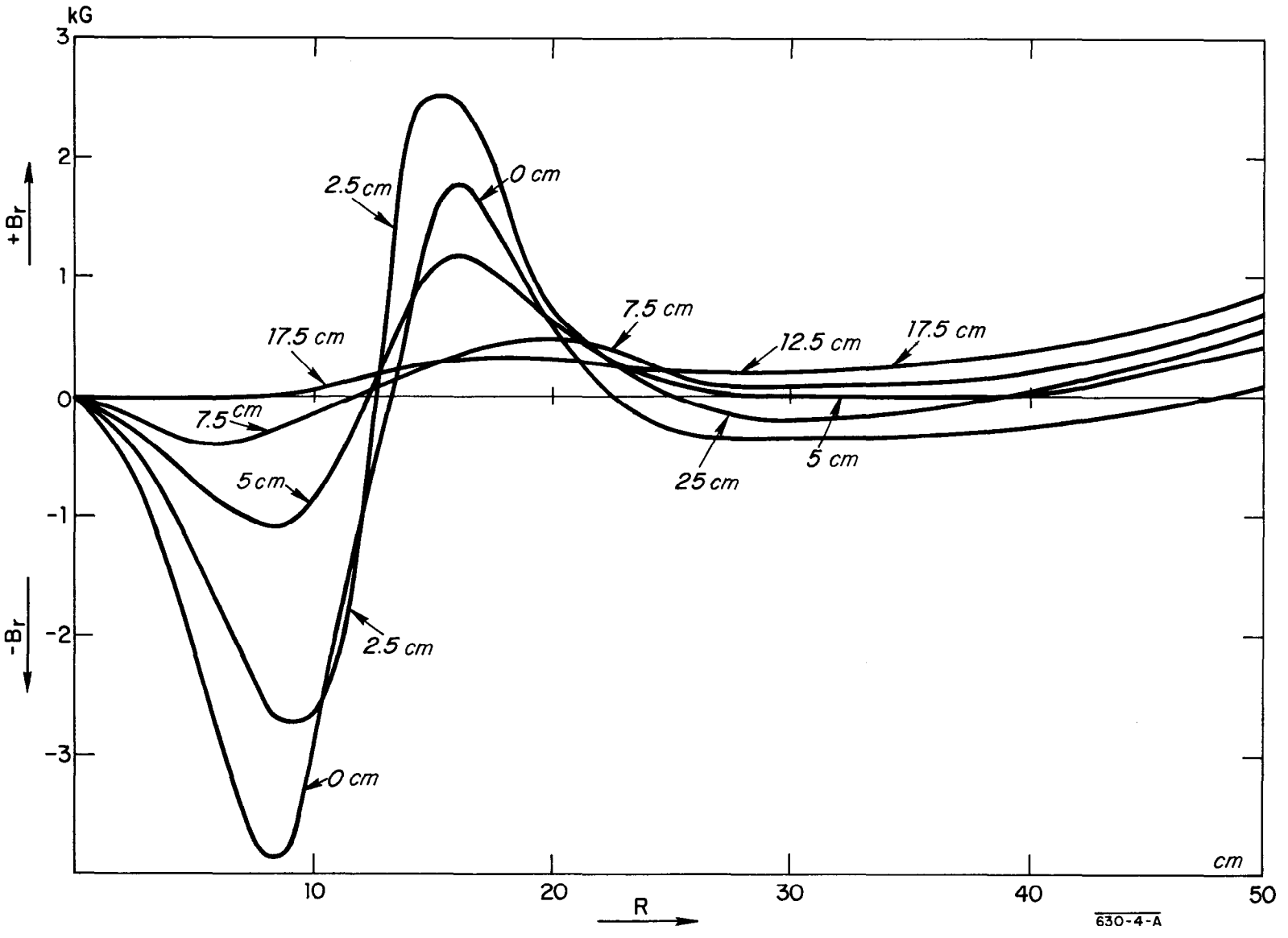

FIG. 2d--Radial field distribution. Magnet provided with 9% Ni-Fe plate.

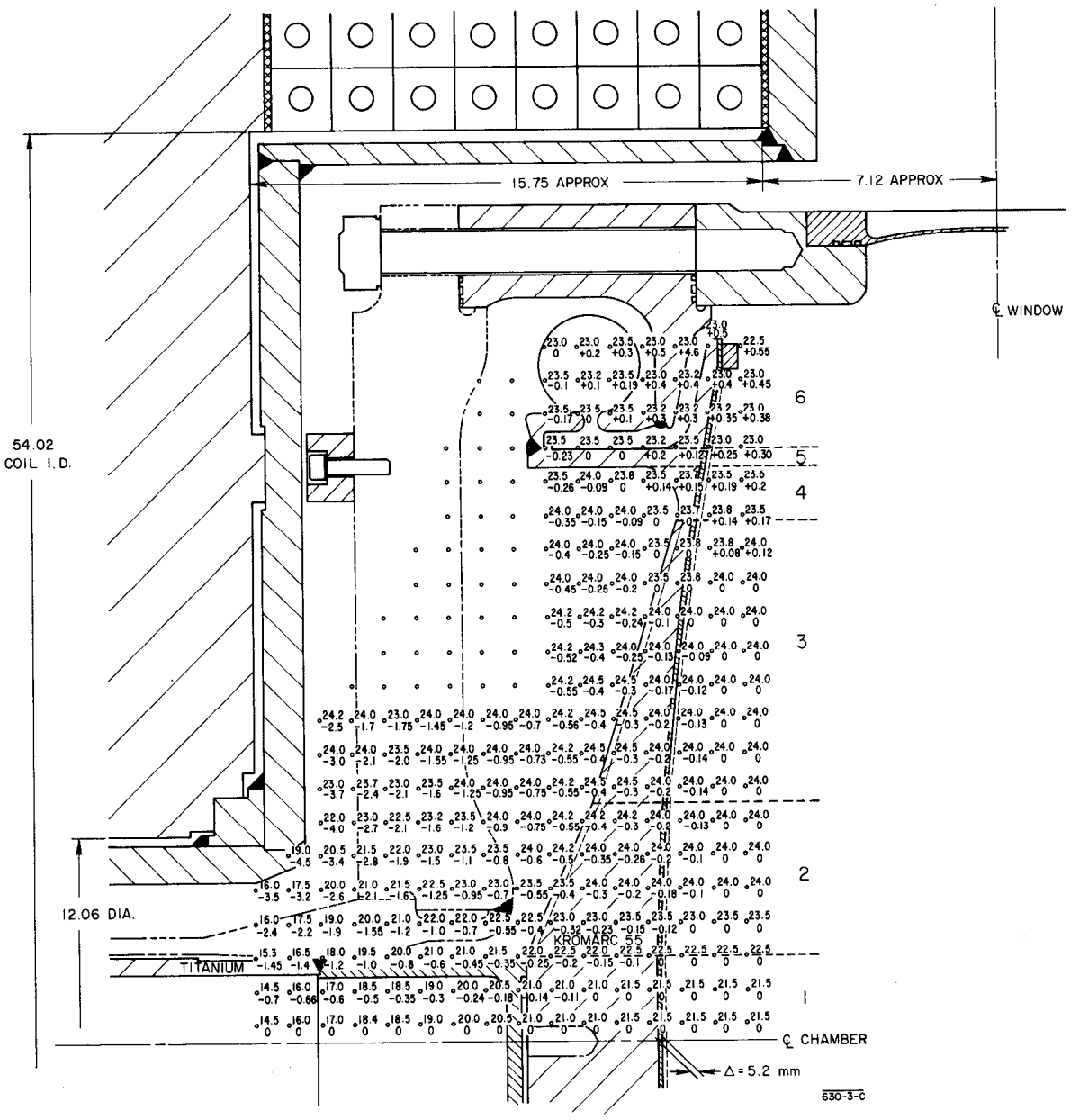

FIG. 3a--Axial and radial field components calculated over the piston. The magnet is not provided with a 9% Ni-Fe ferromagnetic plate. The displacement Δ is 5.2 mm.

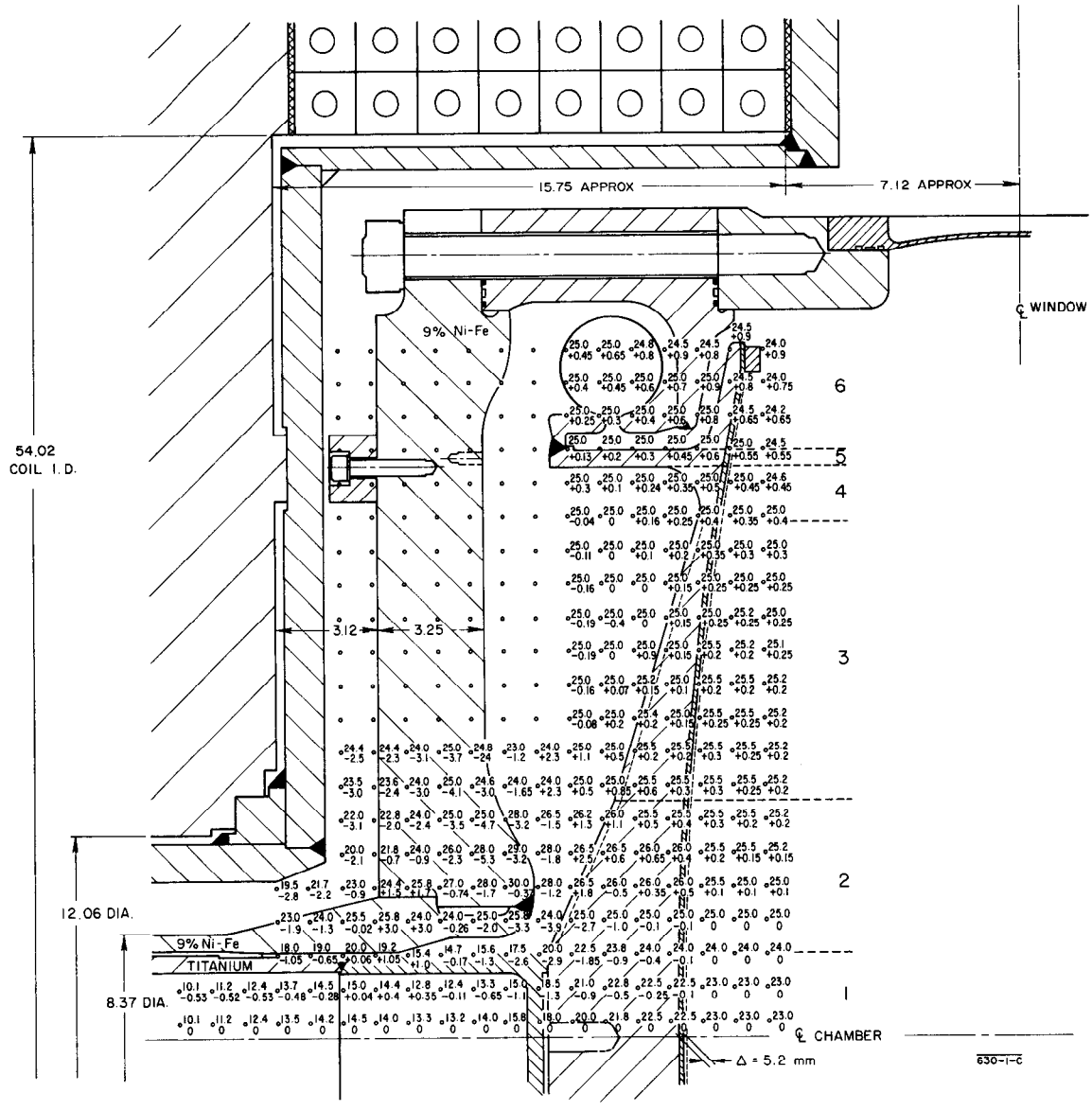

FIG. 3b--Axial and radial field distribution over the piston. The magnet is provided with a 9% Ni-Fe back plate.

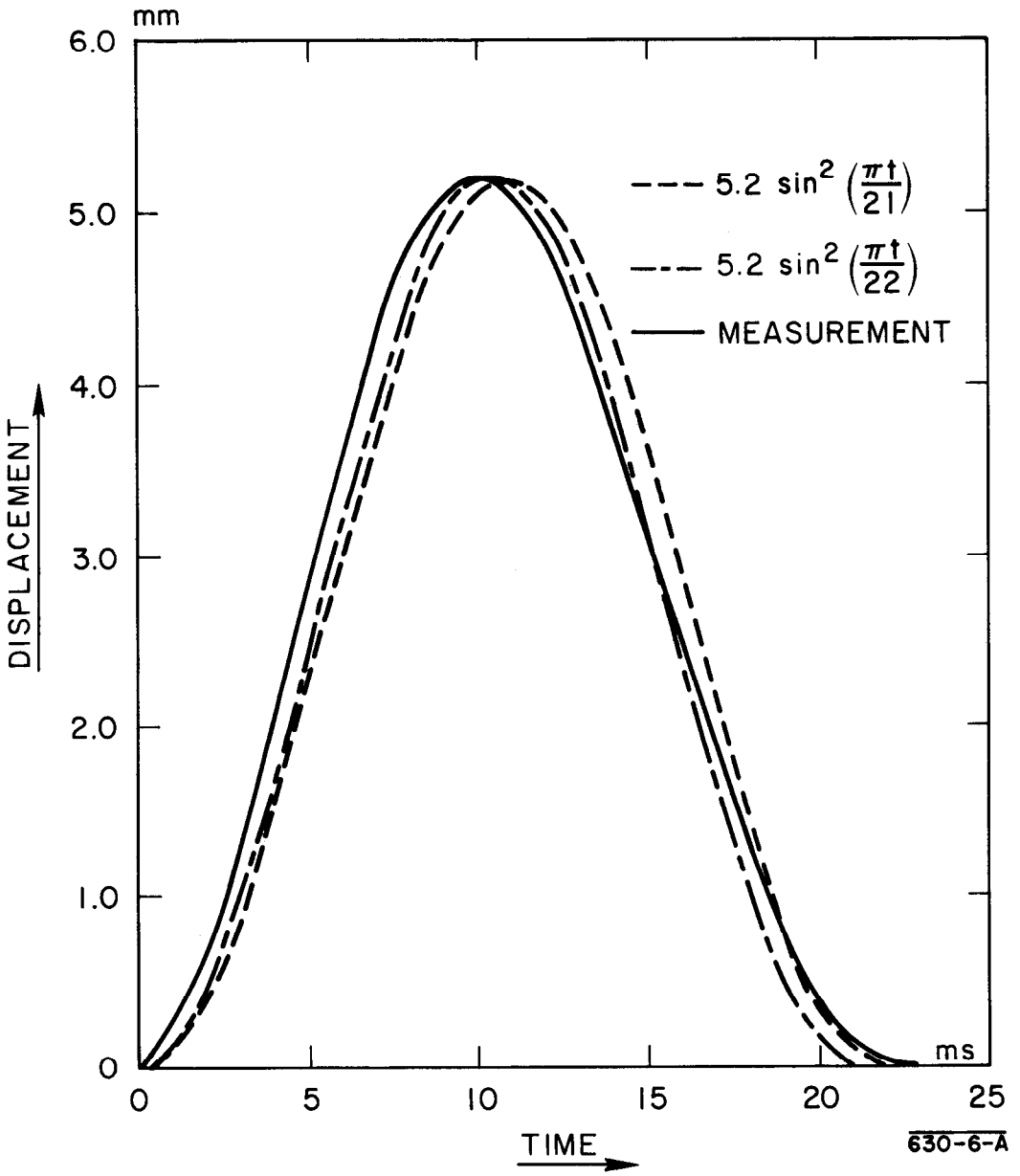

TYPICAL PISTON DISPLACEMENT

FIG. 4--Typical piston displacement.

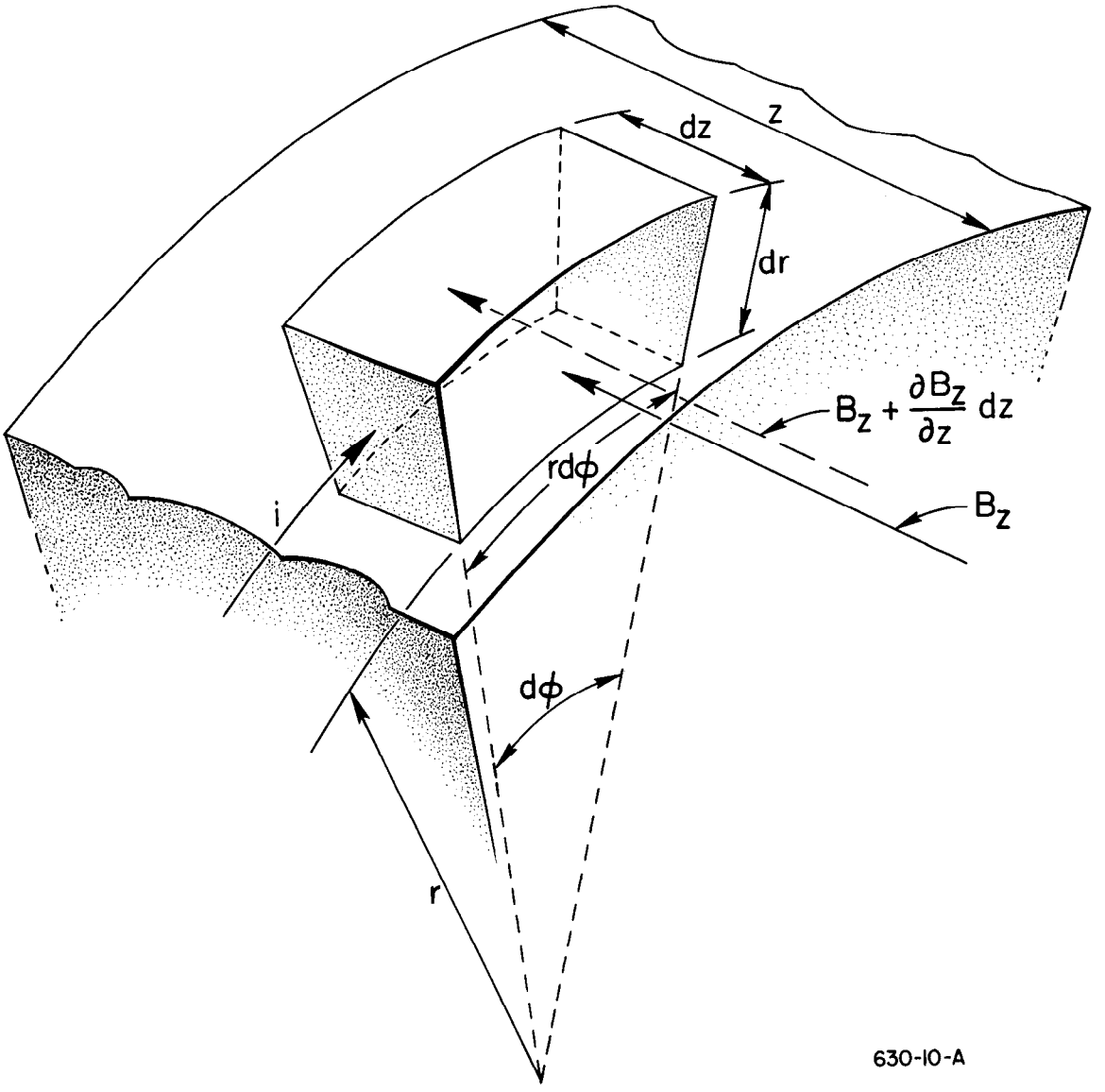

Fig. 5

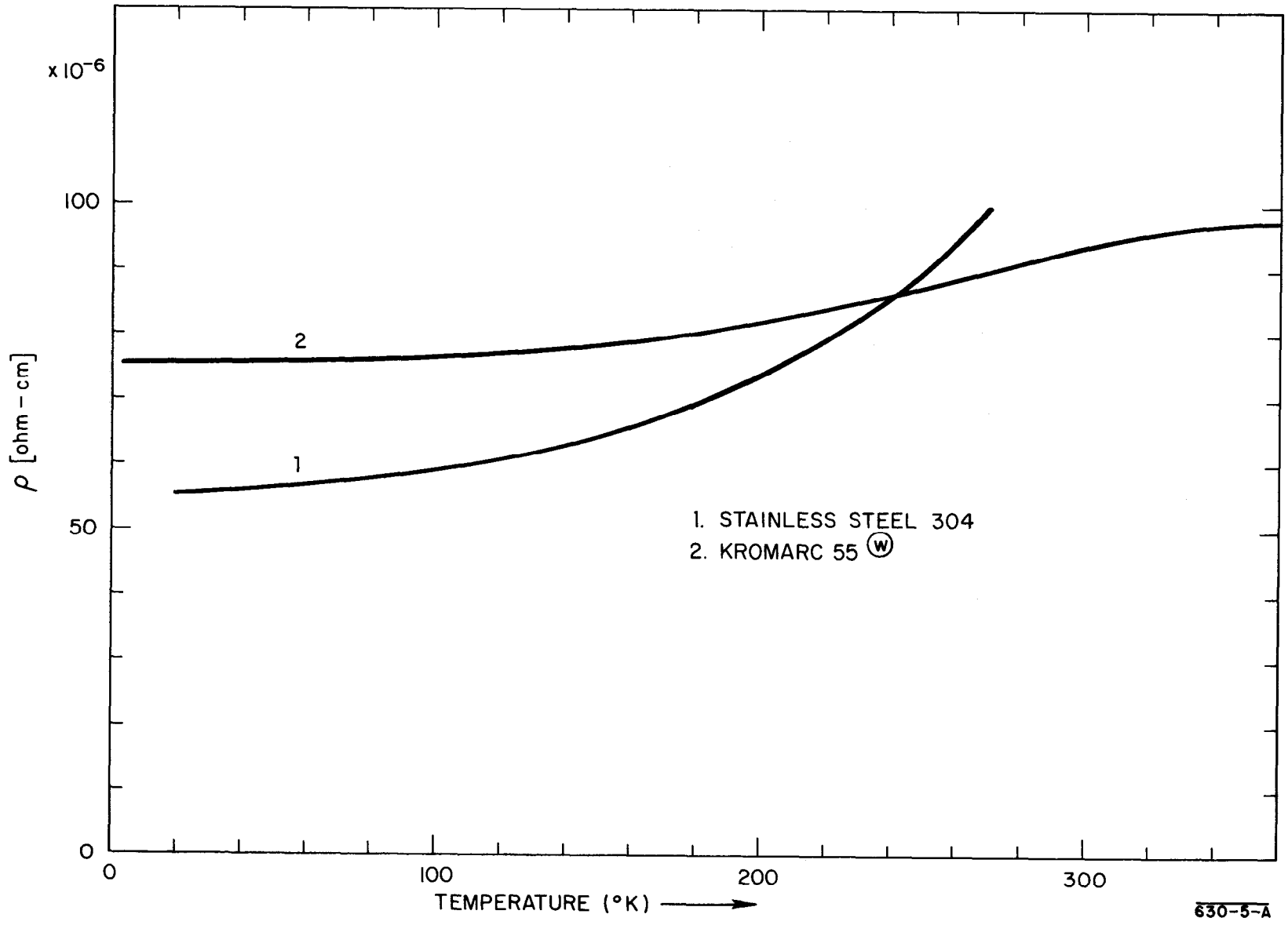

FIG. 6--Resistivity of Kromarc 55 (W) and stainless steel 304 at various temperatures.

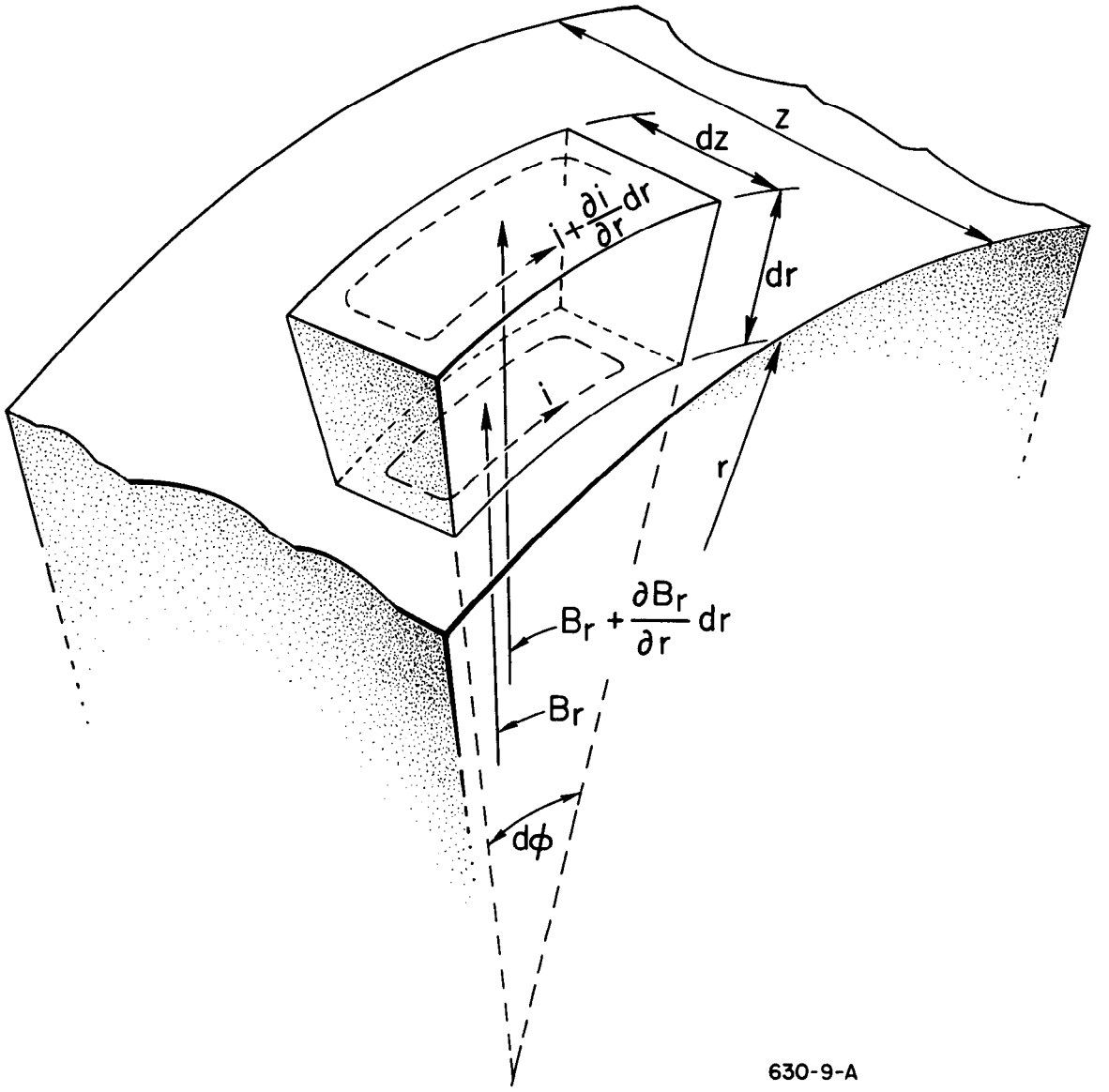
z
dz
$i+\frac{\partial i}{\partial r}dr$
dr
i
r
$B_r+\frac{\partial B_r}{\partial r}dr$
B_r
$d\phi$
630-9-A

Fig. 7